An optoelectronic oscillator for millimeter waves generation based on an integrated optical waveguide ring-resonator

JIAHONG ZHANG[a,b,*], QIBIN CAI[a,b], YINGNA LI[a,b], CHUAN LI[a,b], ZHENGANG ZHAO[a,b]
[a]*Faculty of Information Engineering and Automation, Kunming University of Science and Technology, Kunming 650500, China*
[b]*Yunnan Key Laboratory of Computer Technology Applications, Kunming 650500, China*

An optoelectronic oscillator (OEO) using an integrated optical waveguide ring-resonator (IORR) has been proposed and analyzed. The size of the OEO system is reduced vastly by using an IORR as both optical phase modulator (PM) and filter. The output expression of the radio frequency (RF) signal from the OEO system is theoretically deduced. Simulation results reveal that the RF signal with frequency of 39.16 GHz and side-mode suppression ratio (SMSR) of 54.3 dB can be generated when the radius, attenuation factor, and transmission coefficient of the IORR are designed as 600 μm, 0.66 and 0.63 respectively.

(Received May 31, 2018; accepted June 14, 2019)

Keywords: Microwave photonics, Optoelectronic oscillator (OEO), Integrated optical waveguide, Ring-resonator

1. Introduction

Generation of high quality radio frequency (RF) plays an important role in many application areas such as radar system, wireless communications, radio-over fiber (ROF) system, aerospace, electronic countermeasure, modern instrument et al. The optoelectronic oscillator (OEO) is a well-known solution for generating high-frequency signals with low phase noise comparing with traditional electrical microwave signal generator. Since the first OEO scheme described by Yao and Maleki in 1995 [1, 2], extensive researches have been carried out by many researchers. However, all these researches are mainly focused on increasing the long-term stability [3, 4], reducing the power of the side mode [5, 6, 7], optimizing the phase noise performance [8], increasing the side-mode suppression ratio (SMSR) [9], and increasing the *Q*-factor [10]. Performances of the OEO system or quality of the generated RF signal have been greatly improved. But, as many discrete optical electrical components are required, the structure of current OEO system becomes more complex and the cost increases as well, which limits its practical application. Recently, an OEO with improved tunability is achieved based on a dual-parallel Mach-Zehnder (MZ) modulator embedded with a sub-MZ modulator [11]. Besides, SiO_2 optical waveguide ring resonator (OWRR) is applied to substitute the long fiber-optic delay in order to improve the OEO *Q*-factor and mode selection [12].

In this letter, an OEO based on an integrated optical waveguide Ring-resonator (IORR) has been proposed and investigated. By using an (IORR), both the optical phase modulator (PM) and filter is integrated on a same chip, which makes it possible to reduce size and cost of the system greatly.

2. Operation principles

The diagram of the proposed OEO approach is schematically shown in Fig. 1. The IORR which used as a notch filter is designed and fabricated on *x* cut $LiNbO_3$ substrate by using technologies of photolithography and proton exchange. The modulation electrode is designed and fabricated between the straight waveguide of the IORR to form an optical phase modulator (PM). Besides, the IORR is also used as an energy storage element like the long optical fiber used in traditional OEO system. As a result, because both the optical filter and PM are fabricated on a same chip and the long optical fiber is substituted, size, complexity, and cost of the proposed OEO system are all decreased vastly.

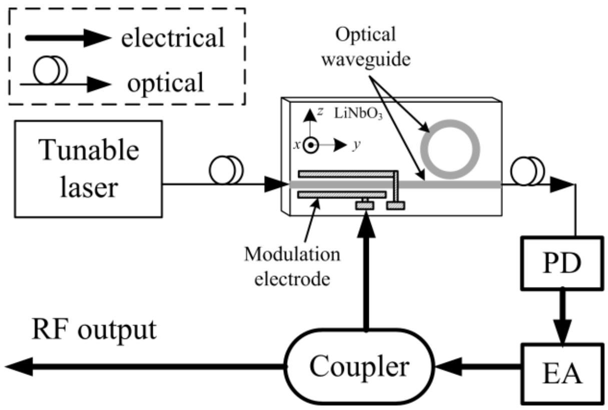

Fig. 1. Schematic diagram of the proposed OEO. (EA, electrical amplifier; PD, photodetector)

By tuning wavelength of the tunable laser, the phase modulation can be work on condition of carrier suppression. The modulated optical field from the IORR can then be theoretically expressed as

$$E_{out1}(t)=E_c e^{j\omega_c t}[\sum_{n=-\infty}^{n=+\infty} j^n J_n(\delta)e^{jn\omega_m t}-kJ_0(\delta)] \quad (1)$$

where, E_c, ω_c are amplitude and frequency of the input optical signal respectively, $J_n(.)$ denotes the first kind of Bessel function at order of n, $\delta=\pi V_m/V_\pi$ is the phase modulation depth, V_m, ω_m are amplitude and frequency of the RF signal, and k is suppression coefficient of the IORR used as a notch filter. The output voltage from the photo-detector (PD) after the electrical amplifier (EA) can then be given by

$$\begin{aligned}V_{out}(t)&=G_A R\rho E_{out}(t)\bullet E_{out}^*(t)\\&=G_A R\rho E_c^2[1-2k\sum_{n=-\infty}^{n=+\infty} j^{2n}J_{2n}(\delta)e^{j2n\omega_m t}+k^2J_0^2(\delta)]\end{aligned} \quad (2)$$

where, G_A is gain of the EA, R, ρ are impedance and responsivity of the PD respectively. Mathematically, in case of small signal modulation, ignoring the higher sidebands and DC components, the output RF signal of the OEO system after many cycles in the closed loop can be expressed as

$$V_{out\_n}(t)\approx E_c^2 e^{j2\omega_m t}\sum_{n=0}^{+\infty}[\underbrace{2G_A R\rho kJ_2(\delta)}_{G}H(\lambda\pm\lambda_m)e^{j2\omega_m(\tau_1+\tau_2)}]^n \quad (3)$$

where, $H(\lambda)=(t^2+\gamma^2-2t\gamma\cos\varphi)/(1+t^2\gamma^2-2t\gamma\cos\varphi)$ is response function of the IORR. $\tau_1=Q_1 n_1\lambda/2\pi c$ is time delay of the light beam travelling through once in the ring cavity, $\tau_2=L_2 n_2/c$ is time delay of the fiber loop, c is the light speed in vacuum, λ is resonance wavelength of the IORR, λ_m corresponding to the side bands of the phase modulation, and L_2, n_2 are length and refractive index of the optical fiber. $Q_1=2n_1\pi R/[\lambda\cos^{-1}(2t\gamma/(1+t^2\gamma^2))]$ is quality factor of the IORR, n_1 is effective refractive index of the optical waveguide, R is radius of the ring cavity, and γ, t are attenuation factor and transmission coefficient of the IORR respectively.

According to Eq. (3), the normalized power of the RF signal from the OEO system can be described as

$$P(\omega_m,t)_n\propto\frac{1}{1-2GH(\lambda\pm\lambda_m)\cos[2\omega_m(\tau_1+\tau_2)]+[GH(\lambda\pm\lambda_m)]^2} \quad (4)$$

where, $\omega_m=2\pi m/(\tau_1+\tau_2)$, ($m$=1, 2, 3, …) is the oscillation frequency of the OEO system.

3. Results and discussions

According to Eq. (4) and the parameters shown in Table 1, response of the IORR is shown in Fig. 2. It can be seen from Fig. 2 that different resonance wavelengths are generated by the designed IORR with different radius. The first resonance wavelengths are 1563.16 nm, 1563.19 nm, 1563.22 nm, and 1563.26 nm respectively for the IORR with radius of 600 μm, 700 μm, 800 μm and 1000 μm. Besides, the second resonance wavelengths for all the designed IORR are 1563.45 μm.

Table 1. Parameters of the proposed OEO system

c	L_2	n_2	n_1	γ	t	k
3×10^8 m/s	1 m	1.5	2.1	0.66	0.63	0.95

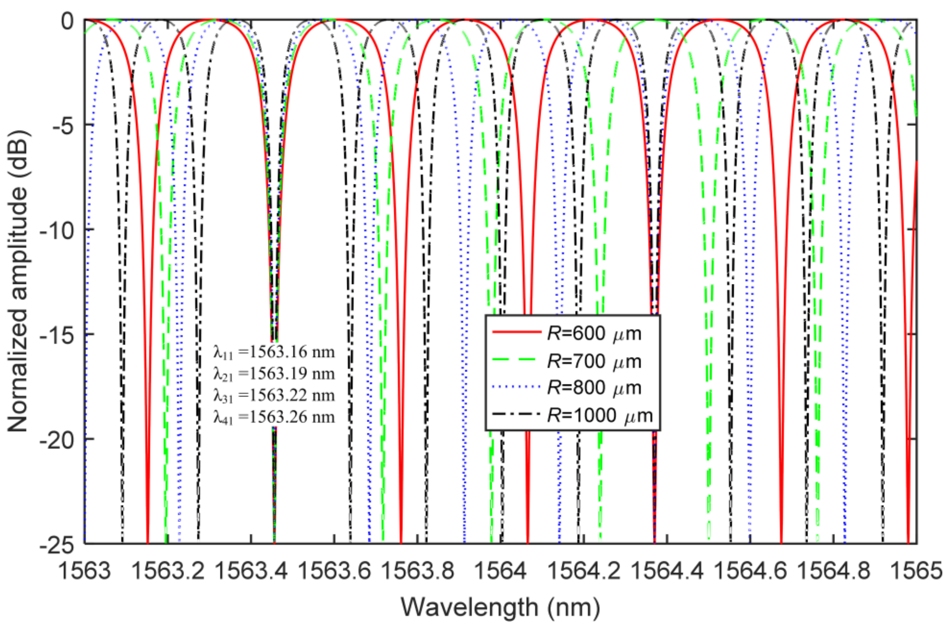

Fig. 2. Response of the designed IORR

Based on the results shown in Fig. 2, the input wavelengths of the OEO system are tuned at 1563.16 nm, 1563.19 nm, 1563.22 nm, 1563.26 nm respectively to make the IORR becomes a notch filter used to suppress the carrier of the optical phase modulation. On this condition, as shown in Fig. 3(a), output RF signals of the OEO system are 21.96 GHz, 28.06 GHz, 31.36 GHz, and 39.16 GHz respectively for the designed IORR with radius of 1000 μm, 800 μm, 700 μm and 600 μm. Moreover, form Fig. 3(b) when the resonance wavelengths of the four designed IORR are all tuned at 1563.45 nm, output RF signals of the OEO system are 21.96 GHz, 27.46 GHz, 31.36 GHz, and 39.26 GHz. As a result, frequencies of the output RF signals are mainly determined by the radius of the designed IORR.

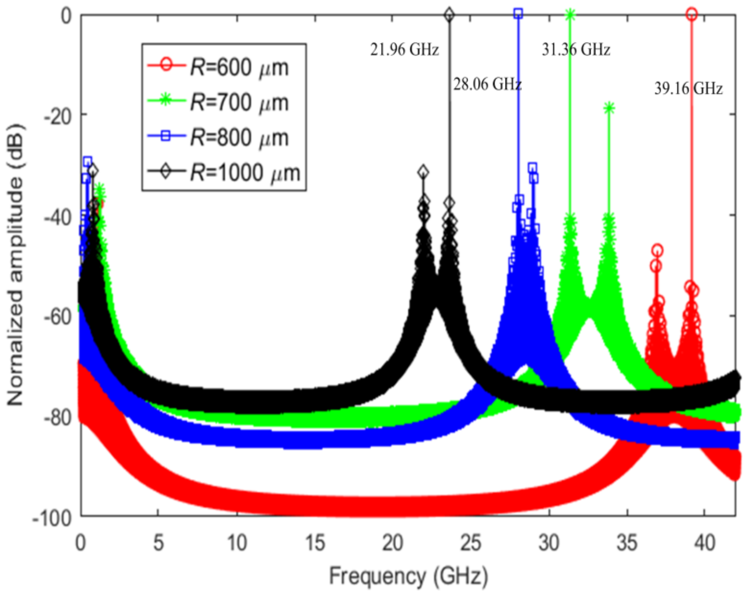

a)

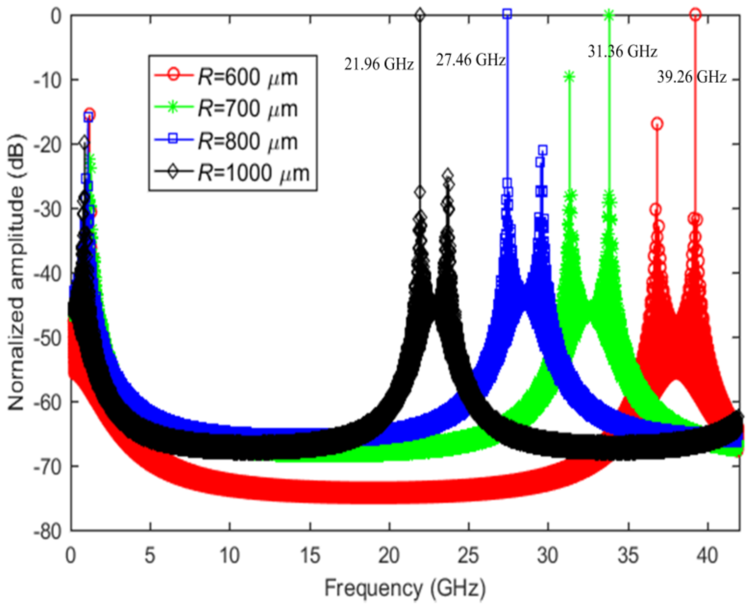

b)

Fig. 3. Output RF signals of the OEO system (a) wavelengths are 1563.16 nm, 1563.19 nm, 1563.22 nm and 1563.26 nm respectively for the four designed IORRs, (b) wavelengths are all 1563.45 nm

Furthermore, Fig. 4 shows output RF signals of the OEO system when the IORR are designed with different attenuation factors γ and transmission coefficients t. It can be seen in Fig. 4(a) that the extinction ratios (ER) are -25 dB, -15 dB, dB, and -13 dB respectively when γ is designed as 0.66, t is designed as 0.63, 0.56, 0.76, and R is

600 μm. Correspondingly, from Fig. 4(b), Fig. 4(c), Fig. 4(d), side-mode suppression ratios (SMSR) of the output RF signals are 34.5 dB, 5.0 dB, and 1.7 dB respectively. Therefore, SMSR of the output RF signal is mainly affected by the designed attenuation factor and transmission coefficient of the IORR.

However, in this paper, the IORR is designed not only on the desired performance but also on current optical waveguide fabrication technology. Consider the mature fabrication technology of $LiNbO_3$ integrated electro optical (EO) modulator, the $LiNbO_3$ IORR with radius, attenuation factor, and transmission coefficient of 600 μm, 0.66 and 0.63 are designed to ensure the practical operability of such OEO system. Accordingly, when designing an IORR chip, to meet the practical requirements, waveguide material, fabrication technology, and simulation results should all be take into account.

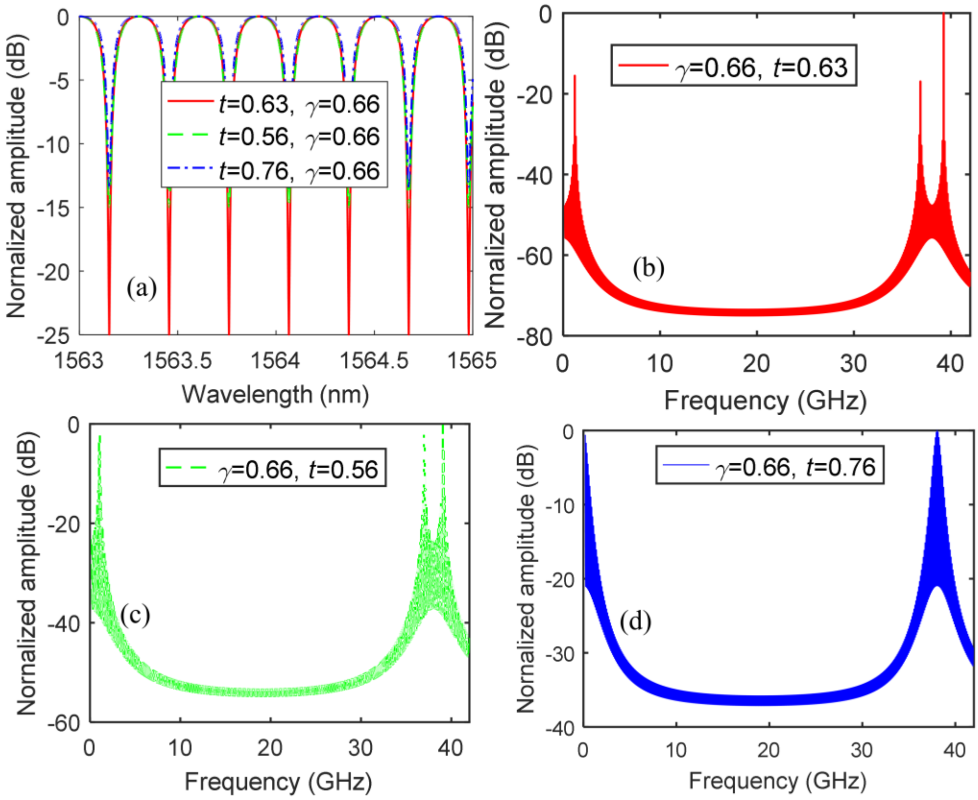

Fig. 4. Output RF signals of the OEO system (a) IORR response for different γ and t; (b) output RF signal as γ=0.66, t=0.63; (c) output RF signal as γ=0.66, t=0.56; (d) output RF signal as γ=0.66, t=0.76

4. Conclusions

In conclusion, a new OEO system is proposed and theoretically demonstrated. By using an IORR as both the optical PM and filter, size and cost of the system can be reduced greatly. When radius, attenuation factor, and transmission coefficient of the IORR are designed as 600 μm, 0.66 and 0.63 respectively, RF signal with frequency and SMSR of 39. 16 GHz and 54.3 dB is generated.

Besides, frequency and SMSR of the output RF signal are mainly determined by the radius *R*, the attenuation factor *γ* and transmission coefficient *t* of the IORR. All the results revel that such OEO approach has potential capability to be used in the foreseeable future for generating of millimeter waves.

Acknowledgement

This work was supported by National Natural Science Foundation of China (Grant No. 61765009), the Applied Basic Research Project of Yunnan province (Grant No. 2018FB106), and the Introducing Talent Research Start-up Project of KMUST (Grant No.KKSY201603042).

References

[1] X. S. Yao, L. Maleki, JPL, Pasadena, CA, USA, TDA Progress Rep. 42-123, (1995).
[2] A. J. Seeds, K. J. Williams, Journal of Lightwave Technology **24**(12), 4628 (2006).
[3] L. Bogataj, M. Vidmar, B. Batagelj, Journal of Lightwave Technology **32**(20), 3690 (2014).
[4] M. Vallet, M. Romanelli, G. Loas, F. V. Dijk, M.

Alouini, IEEE Photonics Technology Letters **28**(10), 1088 (2016).
[5] J. Cho, H. Kim, H. Sung, IEEE Photonics Technology Letters **27**(13), 1391 (2015).
[6] M. Bagnell, J. Davila-Rodriguez, P. Delfyett, Journal of Lightwave Technology **32**(6), 1063 (2014).
[7] A. Liu, J. Liu, J. Dai, Y. Dai, F. Yin, J. Li, IEEE Photonics Technology Letters **29**(19), 1671 (2017).
[8] Z. Zhou, C. Yang, Z. Cao, Y. Chong, X. Li, IEEE Photonics Technology Letters **28**(4), 516 (2016).
[9] L. Bogataj, M. Vidmar, B. Batagelj, IEEE Transactions on Microwave Theory & Techniques **64**(2), 663 (2016).
[10] G. Charalambous, A. Perentos, S. Iezekiel, IEEE Photonics Technology Letters **28**(24), 2850 (2016).
[11] M. Singh, S. Kumar Raghuwanshi, R. K. Bahl, Measurement Science and Technology **29**, 125201 (2018).
[12] J. Chen, Y. Zheng, C. Xue, C. Zhang, Y. Chen, Optics Express **26**(10), 12638 (2018).

*Corresponding author: zjh_mit@163.com